Supporting Information for

Structural Transformation between Rutile and Spinel Crystal Lattices in Ru-Co Binary Oxide Nanotubes: Enhanced Electron Transfer Kinetics for Oxygen Evolution Reaction

Areum Yu, Myung Hwa Kim, Chongmok Lee, Youngmi Lee*

Department of Chemistry and Nano Science, Ewha Womans University, Seoul, 03760, Korea

*Corresponding author: (Fax) +82-2-3277-2384, (E-mail) youngmilee@ewha.ac.kr.

Table S1. Lattice constants of RuO_2 rutile structure and Co_3O_4 cubic structure according to Bragg's law

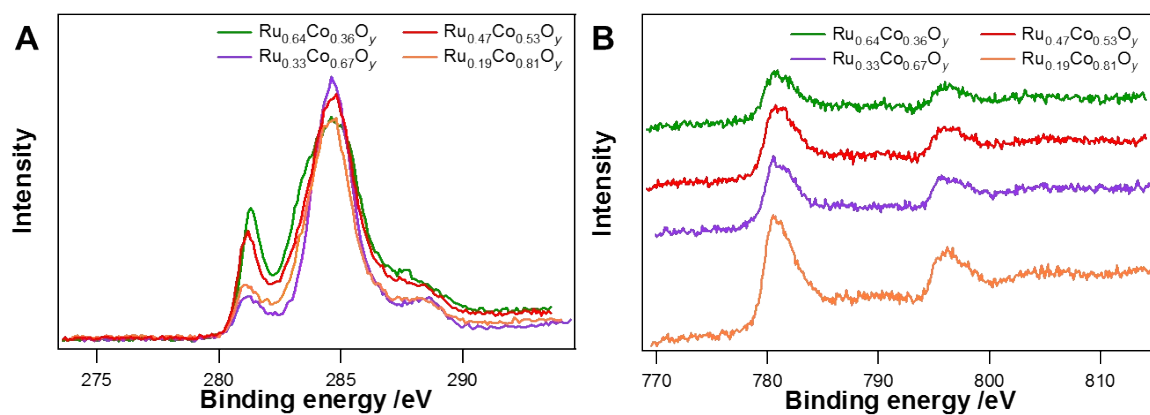| Materials	a (RuO_2, nm)	c (RuO_2, nm)	a (Co_3O_4, nm)
RuO_2	0.4523	0.3116	
$Ru_{0.77}Co_{0.23}O_y$	0.4476	0.3065	
$Ru_{0.64}Co_{0.36}O_y$	0.4475	0.3057	0.8142
$Ru_{0.47}Co_{0.53}O_y$	0.4489	0.3060	0.8123
$Ru_{0.33}Co_{0.67}O_y$	0.4486	0.3058	0.8112
$Ru_{0.19}Co_{0.81}O_y$	0.4496	0.3077	0.8108
Co_3O_4			0.8103

Figure S1. High-resolution XPS spectra of (A) Ru 3d and (B) Co 2p regions of $Ru_xCo_{1-x}O_y$ nanomaterials (x = 0.19, 0.33, 0.47 and 0.64).
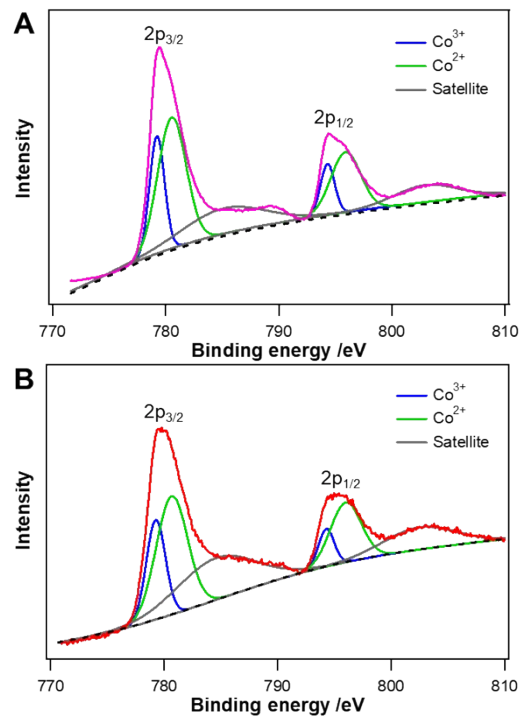
Figure S2. High resolution Co 2p XPS spectra of (A) electrospun Co_3O_4 nanotubes and (B) $Ru_{0.47}Co_{0.53}O_y$ nanotubes. The deconvoluted area ratios of Co^{2+} to Co^{3+} for $2p_{1/2}$ are 2.46 and 3.11 in Co_3O_4 and $Ru_{0.47}Co_{0.53}O_y$ nanotubes, respectively.
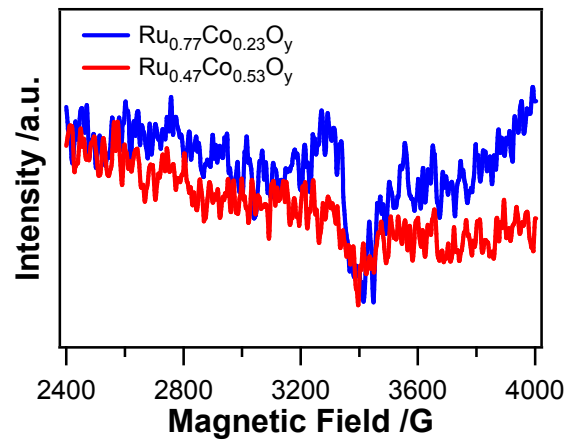
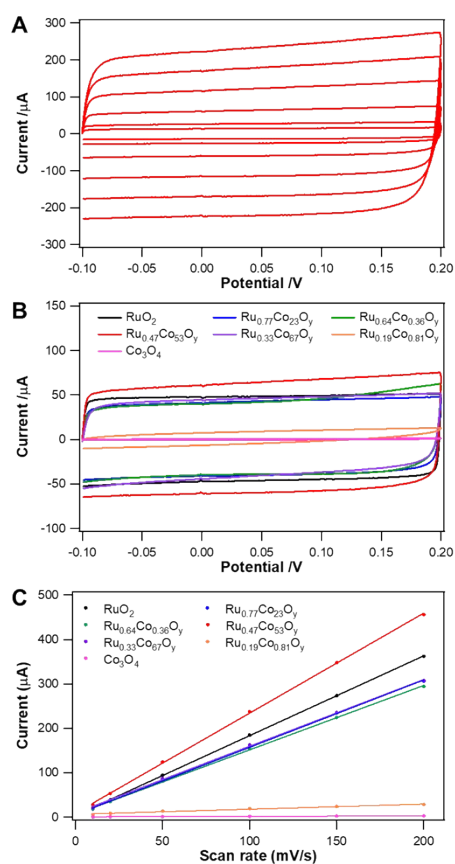**Figure S3.** Electron paramagnetic resonance (EPR) spectra of $Ru_{0.77}Co_{0.53}O_y$ and $Ru_{0.47}Co_{0.53}O_y$.

Figure S4. (A) Cyclic voltammograms of $Ru_{0.47}Co_{0.53}O_y$ in 1.0 M KNO_3 solution at various scan rates of 10, 20, 50, 100, 150, and 200 mV s^{-1}. (B) Cyclic voltammograms of as prepared RuO_2, $Ru_xCo_{1-x}O_y$ ($0 < x < 1$) and Co_3O_4 nanomaterials obtained at a scan rate of 50 mV s^{-1}. (C) Plots of anodic and cathodic current differences (Δi_c) measured at 0.05 V as a function of scan rate.
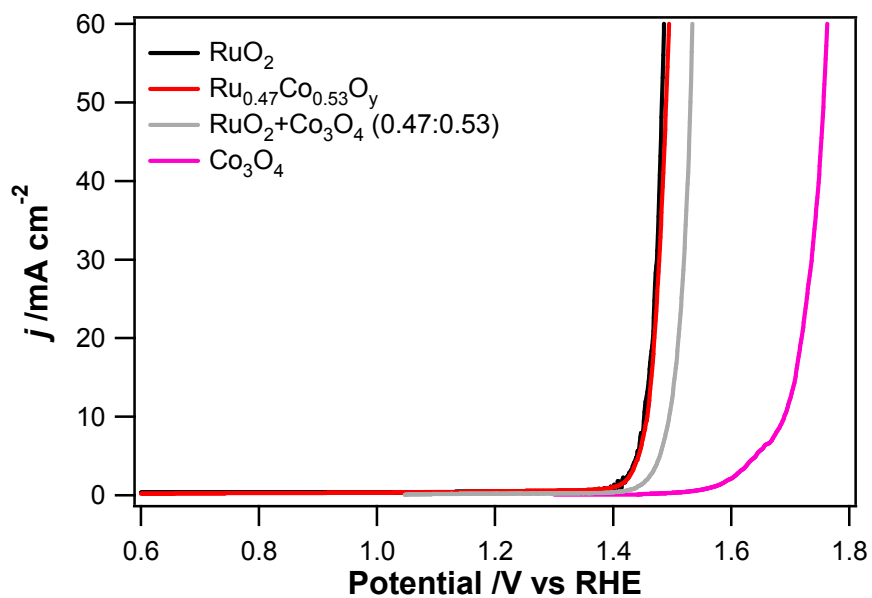
Figure S5. *iR*-compensated RDE voltammograms for OER at RuO_2, $Ru_{0.47}Co_{0.53}O_y$, Co_3O_4 and physically mixed $RuO_2+Co_3O_4$ nanomaterials obtained in Ar-saturated 1.0 M $HClO_4$ with a rotation rate of 1600 rpm at a scan rate of 10 mV s^{-1}.
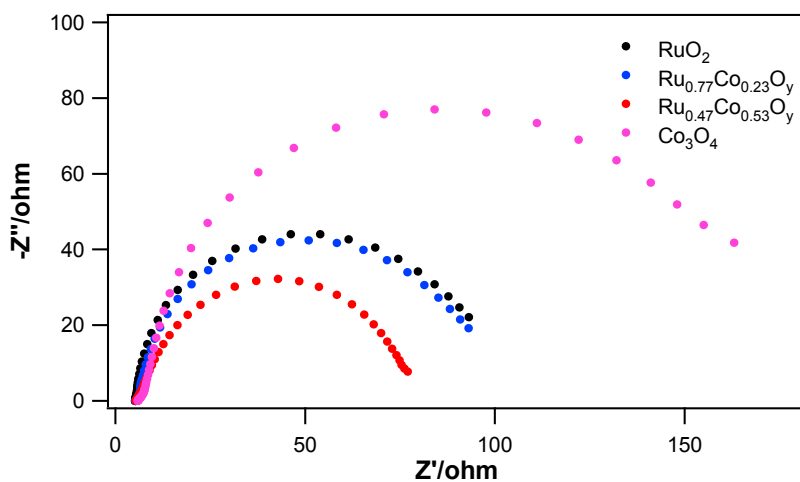
Figure S6. Nyquist plots of RuO_2, $Ru_xCo_{1-x}O_y$ (x = 0.47 and 0.77) and Co_3O_4 nanomaterials measured in 1 M $HClO_4$ solution at potentials achieving 5 mA cm^{-2}.

Table S2. Charge-transfer resistance (R_{ct}) values of RuO_2, $Ru_xCo_{1-x}O_y$ (x = 0.47 and 0.77) and Co_3O_4 nanomaterials measured from the Nyquist plots in Figure S6.

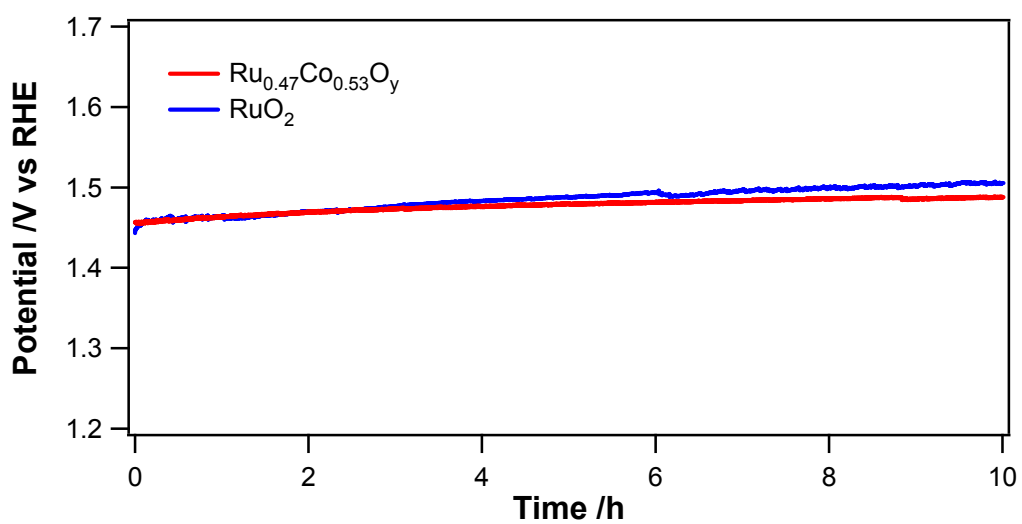| Materials	Resistance (Ω)
RuO_2	90.9
$Ru_{0.77}Co_{0.23}O_y$	86.9
$Ru_{0.47}Co_{0.53}O_4$	68.2
Co_3O_4	155.7

Figure S7. Chronopotentiograms of $Ru_{0.47}Co_{0.53}O_y$ and RuO_2 obtained with a constant applied current of 10 mA cm^{-2} in 0.1 M HClO$_4$ aqueous solution. Electrodes were not mechanically rotated.
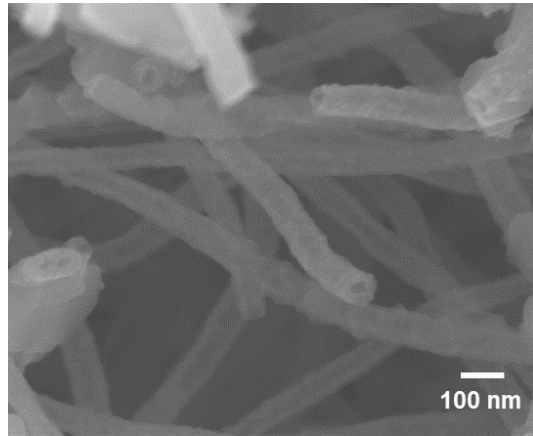
Figure S8. A SEM image of $Ru_{0.47}Co_{0.53}O_y$ nanotubes after the continuous OER at 10 mA cm^{-2} for 8 000 s.

Table S3. Comparison of the atomic ratio in $Ru_{0.47}Co_{0.53}O_y$ before and after the continuous OER at 10 mA cm^{-2} for 8 000 s which were determined with SEM-EDS measurements at more than 20 different locations.

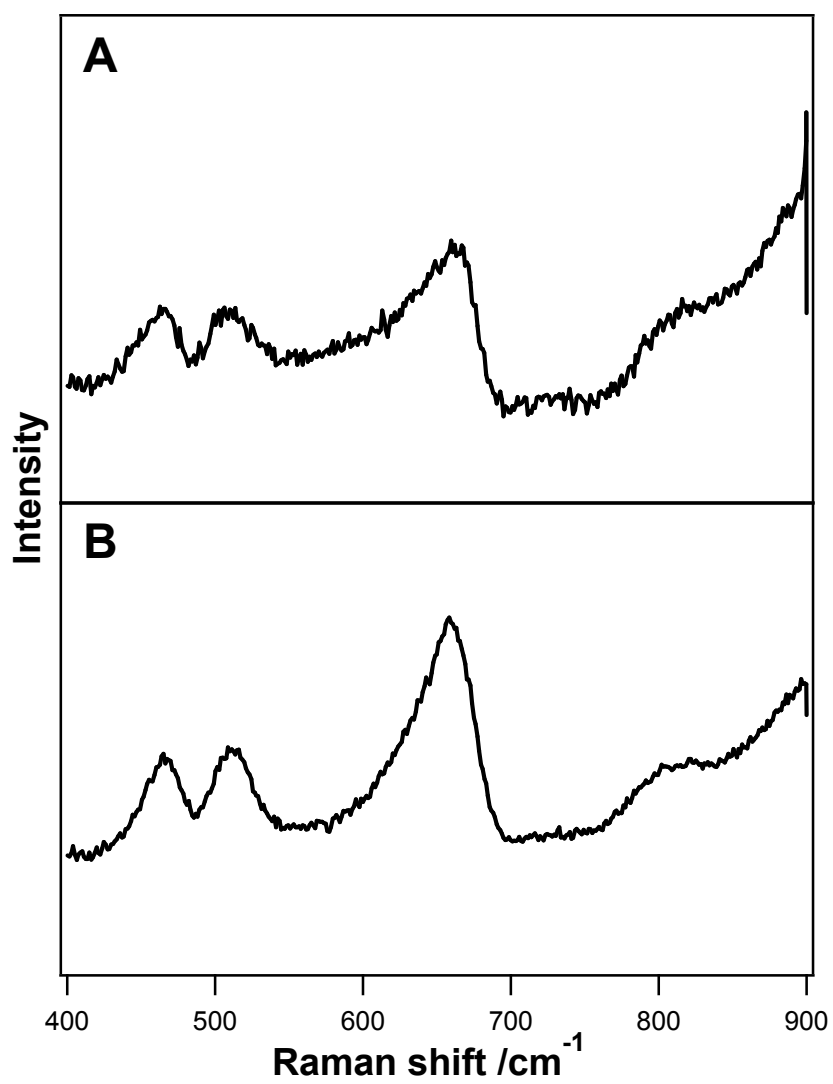| Materials	Elements	Atomic Ratio (%)
$Ru_{0.47}Co_{0.53}O_y$ before stability test	Ru	46.9 ($\pm$ 1.6)
	Co	53.1 ($\pm$ 1.6)
$Ru_{0.47}Co_{0.53}O_y$ after stability test	Ru	46.7 ($\pm$ 2.2)
	Co	53.3 ($\pm$ 2.2)

Figure S9. Raman spectra for $Ru_{0.46}Co_{0.53}O_y$ nanotubes (A) before and (B) after a stability test with a constant applied current of 10 mA cm^{-2} for 3600 s.
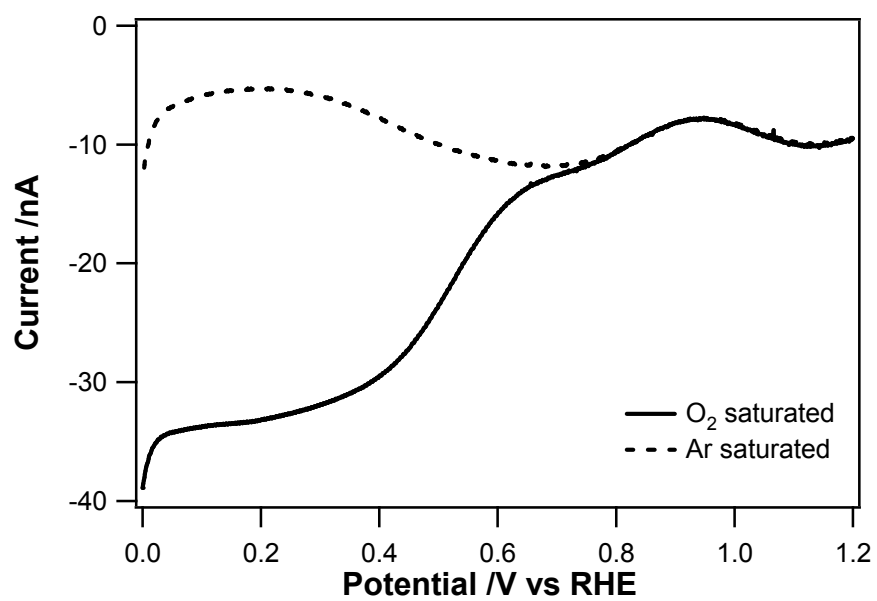
Figure S10. LSV for O_2 reduction in O_2-saturated and Ar-saturated 1.0 M $HClO_4$ solution at a Pt tip electrode (25 μm in diameter) with a scan rate of 10 mV s^{-1}.